

Polarization-Dependent Optical Forces Arising from Fano Interference

Yao Zhang,* Tianyue Li, Shuming Wang,* Zhenlin Wang, and Shining Zhu

A Fano resonance originates from the resonant coupling between interacting multipoles inside nanostructures. It breaks the symmetry of spectral line shape and enables Fano-resonant media to present unusual scattering properties. However, understanding the mechanical effects of such multipolar coupling systems is highly complex compared with the traditional simple dipole. In this work, using single Si nanospheres as the Fano-resonant media, optical forces arising from different types of Fano resonances including the electric, magnetic, and magnetoelectric Fano resonances are investigated. It is shown that the directions of these types of forces are tunable in three dimensions. The necessary condition to realize a direction change of the Fano-resonance-induced forces and elucidate the underlying physics are presented. Furthermore, it is found that the Fano-resonance-induced forces exhibit strong polarization-dependent properties which traditional optical (dipolar) forces cannot possess.

1. Introduction

The radiative interaction between two multipoles results in a Fano resonance.^[1–3] An electric Fano resonance (EFR) is generated by the interaction between electric multipoles which exist in plasmonic nanomaterials.^[4] Magnetic multipoles are generally present in “artificial magnetic” structures or high-index dielectric nanomaterials such as Si nanospheres.^[5–7] The interaction between the magnetic multipoles leads to a magnetic Fano resonance (MFR). Significant MFR or EFR can produce unique scattering properties, rendering Fano-resonant media particularly attractive for the development of chemical or biological sensors and optical antenna or switching.^[2] Similarly, the magnetic

multipoles can interact with the electric multipoles, thereby generating a magnetoelectric Fano resonance (MEFR).^[8–10] Nanostructures that support MEFR have been used for achieving unidirectional scattering of light, which provides an efficient method for controlling light at nanoscale and is important for light-on-chip integration.^[1,8–10] They are also exploited for advanced optical manipulation, by harnessing the extraordinary optical momenta, including the Belinfante’s spin momentum and imaginary Poynting momentum.^[5,7,11–14]

Since the Fano-resonant media can distinctively tailor the scattered light, it should experience an unusual optical force in response to the Fano resonance. Recently, several studies have been performed on the Fano resonance force for a variety of Mie nanostructures.^[6,7,10,15–17] The force has also been explored for pulsed light, by considering the nonlinear effects induced in the materials.^[18–20] It shows that the total optical force is sensitive to the light wavelength and the size of the nanostructures. In this letter, we offer a distinct perspective for the Fano resonance forces, by highlighting their dependence on the phase difference between interacting multipoles and on the polarization of a linearly polarized light. While the direction of polarization is usually associated to the optical torque on asymmetric structures,^[21] we show that this fundamental characteristic of light controls also the Fano resonance forces on isotropic homogeneous spheres. Interestingly, the EFR, MFR, and MEFR forces exhibit different dependence on the polarization direction.

2. Results

As single Si nanospheres (SiNSs) support both electric and magnetic multipoles,^[4–7] we use SiNSs of different sizes as the

Y. Zhang
 Institute of Nanophotonics
 Jinan University
 Guangzhou 511443, China
 E-mail: zhyao5@jnu.edu.cn

Y. Zhang
 Key Laboratory of Optoelectronic Information and Sensing Technologies
 of Guangdong Higher Education Institutes
 Jinan University
 Guangzhou 510632, China

T. Li, S. Wang, Z. Wang, S. Zhu
 National Laboratory of Solid-State Microstructures
 Collaborative Innovation Center for Advanced Microstructures
 School of Physics
 Nanjing University
 Nanjing 210093, China
 E-mail: wangshuming@nju.edu.cn

S. Wang, S. Zhu
 Key Laboratory of Intelligent Optical Sensing and Manipulation Ministry
 of Education
 Nanjing University
 Nanjing 210093, China

The ORCID identification number(s) for the author(s) of this article can be found under <https://doi.org/10.1002/apxr.202200048>

© 2023 The Authors. Advanced Physics Research published by Wiley-VCH GmbH. This is an open access article under the terms of the Creative Commons Attribution License, which permits use, distribution and reproduction in any medium, provided the original work is properly cited.

DOI: 10.1002/apxr.202200048

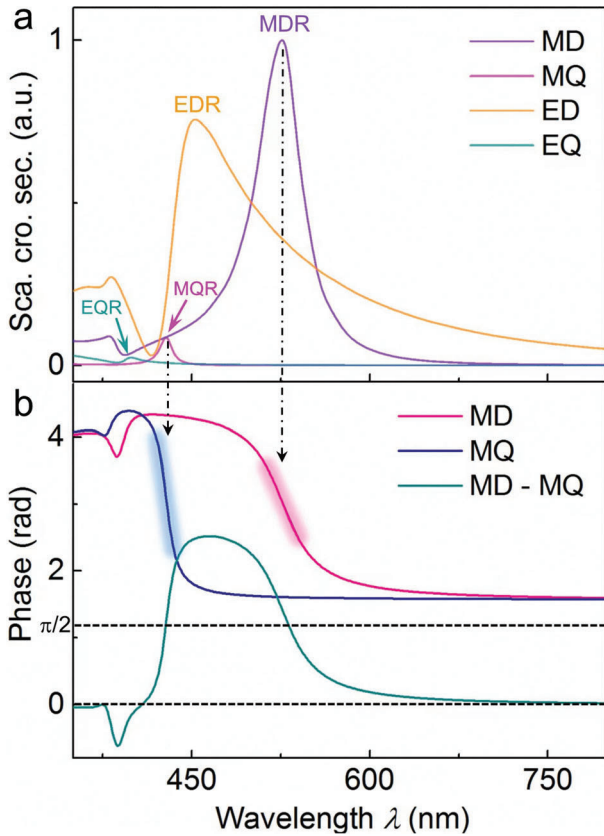


Figure 1. Multipoles inside a Si nanosphere (diameter: 120 nm) in water. a) Partial scattering spectra contributed by a magnetic dipole (MD), a magnetic quadrupole (MQ), an electric dipole (ED), and an electric quadrupole (EQ), respectively, as calculated via the Mie theory. b) Oscillating phases of and phase difference between MD and MQ.

Fano-resonant media, with a permittivity of Si adapted from Ref. [22]. Insight into the multipoles in a SiNS can be gained from **Figure 1**, which shows the scattering cross-section C_{sca} of the SiNS (nominal diameter: 120 nm) in water, as determined via the Mie theory^[23]

$$C_{sca} = \frac{1}{k^2 |\mathbf{E}_0^{inc}|^2} \sum_{l=1}^N \sum_{m=-l}^l (|p_{l,m}|^2 + |q_{l,m}|^2) \quad (1)$$

where $|\mathbf{E}_0^{inc}|^2$ is the incident intensity, k is the wave number in water, $p_{l,m}$ and $q_{l,m}$ denote the scattering coefficients associated with magnetic and electric multipolar contributions, respectively. Partial scattering spectra contributed by a magnetic dipole (MD), a magnetic quadrupole (MQ), an electric dipole (ED), and an electric quadrupole (EQ) are shown while higher-order contributions are negligible. A magnetic dipolar resonance (MDR) occurs at a wavelength $\lambda = 526$ nm and an electric dipolar resonance (EDR) occurs at $\lambda = 453$ nm. In the short-wavelength region, a magnetic quadrupolar resonance (MQR) and an electric quadrupolar resonance (EQR) occur at $\lambda = 428$ and 408 nm, respectively. Near the multipolar resonance, the phase of the corresponding mul-

tipole is extremely sensitive to the light wavelength. Figure 1b plots the phases of the MD and the MQ, as well as their phase difference. When the light wavelength passes through the MDR, the phase of the MD changes abruptly by ≈ 2 rad, but the phase of the MQ (with resonance MQR spectrally separated from the MDR) is almost constant. During this process, both multipoles can oscillate with mutually orthogonal phases, i.e., with an MD–MQ phase difference of $\pi/2$. Similarly, near the MQR, the phases of the MD and the MQ can also be mutually orthogonal. Additionally, the two multipoles can oscillate in phase, i.e., with a phase difference of zero, at the blue side of the MQR. As will be shown below, these two-phase relationships play an important role in determining the direction of each Fano-resonance-induced force.

The total time-averaged optical force acting on the SiNS can be calculated by the integral of time-averaged Maxwell stress tensor,^[24] or the real part of Nieto–Xu equation^[25]

$$F_i = \int_S \text{Re}(T_{ij}) n_j dS \quad (2)$$

where n_j denotes a component of a vector normal to the integration surface S and $T_{ij} = [\epsilon E_i^* E_j + B_i B_j^* - \delta_{ij}(\epsilon |\mathbf{E}|^2 + |\mathbf{B}|^2)]/4\pi$. Note that the electric and magnetic fields, \mathbf{E} and \mathbf{B} , correspond to the total electromagnetic field that includes both the incident and scattered fields. Using the generalized Lorenz–Mie theory,^[26] the incident field can be expanded in terms of vector spherical wavefunctions (VSWFs) as follows

$$\mathbf{E}_{inc} = \sum_{l=1}^{l_{max}} \sum_{m=-l}^l a_{lm} \mathbf{M}_{lm}^{(1)} + b_{lm} \mathbf{N}_{lm}^{(1)} \quad (3)$$

where $\mathbf{M}_{lm}^{(1)}$ and $\mathbf{N}_{lm}^{(1)}$ are VSWFs characterized by spherical Bessel functions, and the expansion coefficients a_{lm} and b_{lm} are determined by the parameters of the incident field. The scattered field can also be expanded

$$\mathbf{E}_{inc} = \sum_{l=1}^{l_{max}} \sum_{m=-l}^l a_{lm} \mathbf{M}_{lm}^{(1)} + b_{lm} \mathbf{N}_{lm}^{(1)} \quad (4)$$

where $\mathbf{M}_{lm}^{(3)}$ and $\mathbf{N}_{lm}^{(3)}$ are VSWFs based on spherical Hankel functions of the first kind, and the scattering coefficients p_{lm} and q_{lm} are linked to a_{lm} and b_{lm} via Mie coefficients P_l and Q_l

$$\begin{aligned} p_{lm} &= P_l a_{lm} = |P_l| |a_{lm}| \exp[i(\phi_l + \alpha_{lm})], \quad q_{lm} = Q_l b_{lm} \\ &= |Q_l| |b_{lm}| \exp[i(\phi_l + \beta_{lm})] \end{aligned} \quad (5)$$

where ϕ_l , α_{lm} , and β_{lm} denote the phases for P_l , Q_l , a_{lm} , and b_{lm} , respectively. Note that for nonabsorbing particles, the phase and modulus of the Mie coefficients are related, so that P_l and Q_l can be expressed in terms of single variables.^[9,27,28]

Substituting Equations (3) and (4) into Equation (2) and applying numerous recursions, product, and the orthogonality of the VSWFs yields the z component of the total optical force acting on a nanosphere in water^[26]

$$F_z = -\frac{\epsilon}{8\pi k^2} \sum_{l=1}^{l_{\max}} \sum_{m=-l}^l \left\{ \text{Im}(2p_{l+1,m} p_{lm}^* + p_{l+1,m} a_{lm}^* + a_{l+1,m} p_{lm}^* + 2q_{l+1,m} q_{lm}^* + q_{l+1,m} b_{lm}^* + b_{l+1,m} q_{lm}^*) \frac{\sqrt{l(l+2)}}{l+1} \sqrt{\frac{(l+m+1)(l-m+1)}{(2l+1)(2l+3)}} - \text{Re}(a_{lm} q_{lm}^* + p_{lm} b_{lm}^* + 2p_{lm} q_{lm}^*) \frac{m}{l(l+1)} \right\} \quad (6)$$

where ϵ is the dielectric constant of water. We can readily determine the Fano-resonance-induced force that is composed of the products of the scattering coefficients. This force can be written as the sum of three terms

$$F_{\text{Fano}} = F_{\text{EFR}} + F_{\text{MFR}} + F_{\text{MEFR}} \quad (7)$$

where

$$F_{\text{EFR}} = -\frac{\epsilon}{4\pi k^2} \sum_{l=1}^{l_{\max}} \sum_{m=-l}^l |Q_{l+1}| |Q_l| |b_{l+1,m}| |b_{lm}| \sin(\Delta\phi_{l+1,l} + \Delta\beta_{l+1,lm}) \frac{\sqrt{l(l+2)}}{l+1} \sqrt{\frac{(l+m+1)(l-m+1)}{(2l+1)(2l+3)}} \quad (8)$$

$$F_{\text{MFR}} = -\frac{\epsilon}{4\pi k^2} \sum_{l=1}^{l_{\max}} \sum_{m=-l}^l |P_{l+1}| |P_l| |a_{l+1,m}| |a_{lm}| \sin(\Delta\phi_{l+1,l} + \Delta\alpha_{l+1,lm}) \frac{\sqrt{l(l+2)}}{l+1} \sqrt{\frac{(l+m+1)(l-m+1)}{(2l+1)(2l+3)}} \quad (9)$$

and

$$F_{\text{MEFR}} = \frac{\epsilon}{4\pi k^2} \sum_{l=1}^{l_{\max}} \sum_{m=-l}^l |P_l| |Q_l| |a_{lm}| |b_{lm}| \cos(\Delta\gamma_l + \Delta\chi_{lm}) \frac{m}{l(l+1)} \quad (10)$$

Note that we have expressed the scattering coefficients in terms of the Mie coefficients using Equation (5), and the phase differences are given by

$$\Delta\phi_{l+1,l} = \varphi_{l+1} - \varphi_l, \Delta\phi_{l+1,l} = \phi_{l+1} - \phi_l, \Delta\gamma_l = \phi_l - \varphi_l, \Delta\beta_{l+1,lm} = \beta_{l+1,m} - \beta_{lm}, \Delta\alpha_{l+1,lm} = \alpha_{l+1,m} - \alpha_{lm}, \Delta\chi_{lm} = \alpha_{lm} - \beta_{lm} \quad (11)$$

The symbols used in this work are summarized in **Table 1**. The MFR-induced force F_{MFR} and the EFR-induced force F_{EFR} originate from the products of multipoles of the same type with adjacent orders, whereas the MEFR-induced force F_{MEFR} is derived from the products of the magnetic and electric multipoles with the same order. For a given incident field, the phase differences $\Delta\beta_{l+1,lm}$, $\Delta\alpha_{l+1,lm}$, and $\Delta\chi_{lm}$ are fixed, so the directions of F_{EFR} , F_{MFR} , and F_{MEFR} are just determined by the phase differences between corresponding interacting multipoles ($\Delta\phi_{l+1,l}$, $\Delta\phi_{l+1,l}$, and $\Delta\gamma_l$). Equations (8)–(10) not only give us ways to calculate the three types of forces that are based on distinct Fano resonances, but their cumulative forms also reveal the force contribution from multipoles with specific orders. For example, by setting $l = 1$ in Equations (9) and (10), one can obtain F_{MFR} and F_{MEFR}

originating from a dipole-quadrupole MFR and a dipolar MEFR, respectively.

Figure 2 shows the wavelength dependence of the Fano-resonance-induced forces and the phase differences of the interacting multipoles for different-sized SiNSs. The forces along the axial (left panels) and transverse (right panels) directions are calculated by applying two different illumination systems based on a TEM₀₀ Gaussian beam (N.A. = 1.2) of linear polarization, as il-

lustrated in insets I and II. In inset I, the SiNS is placed at the focus center of x -polarized light propagating along $+z$ direction, so that the forces in the z direction represent the axial forces. We investigate the transverse forces via 90° rotation of the coordinate system. In this case (see inset II), the light propagates along the $+x$ direction with polarization along the z axis and therefore, the forces in the z direction are actually the transverse forces. To generate nonzero transverse forces, the SiNS is placed on the focal plane, but is deviated from the axis by a displacement $\Delta z = w_0/2$ along the $+z$ direction (where w_0 is the beam waist). Here, F_{MFR} , F_{MEFR} , and F_{EFR} considered here are derived from the MD–MQ, MD–ED, and ED–EQ interactions (insets III–VI), respectively. In

Table 1. List of the quantities and corresponding symbols used in the paper.

Quantities	Symbols (mag., elec.)	Symbols for phase	Phase difference
Mie coefficients	P_l, Q_l	ϕ_l, φ_l	$\Delta\phi_{l+1,l} = \varphi_{l+1} - \varphi_l$ $\Delta\phi_{l+1,l} = \phi_{l+1} - \phi_l$ $\Delta\gamma_l = \phi_l - \varphi_l$
IF coefficients	a_{lm}, b_{lm}	α_{lm}, β_{lm}	$\Delta\beta_{l+1,lm} = \beta_{l+1,m} - \beta_{lm}$ $\Delta\alpha_{l+1,lm} = \alpha_{l+1,m} - \alpha_{lm}$ $\Delta\chi_{lm} = \alpha_{lm} - \beta_{lm}$
SF coefficients	p_{lm}, q_{lm}	–	–

IF, incident field; SF, scattered field. The phase of SF coefficients are determined by the phase of both the Mie and IF coefficients.

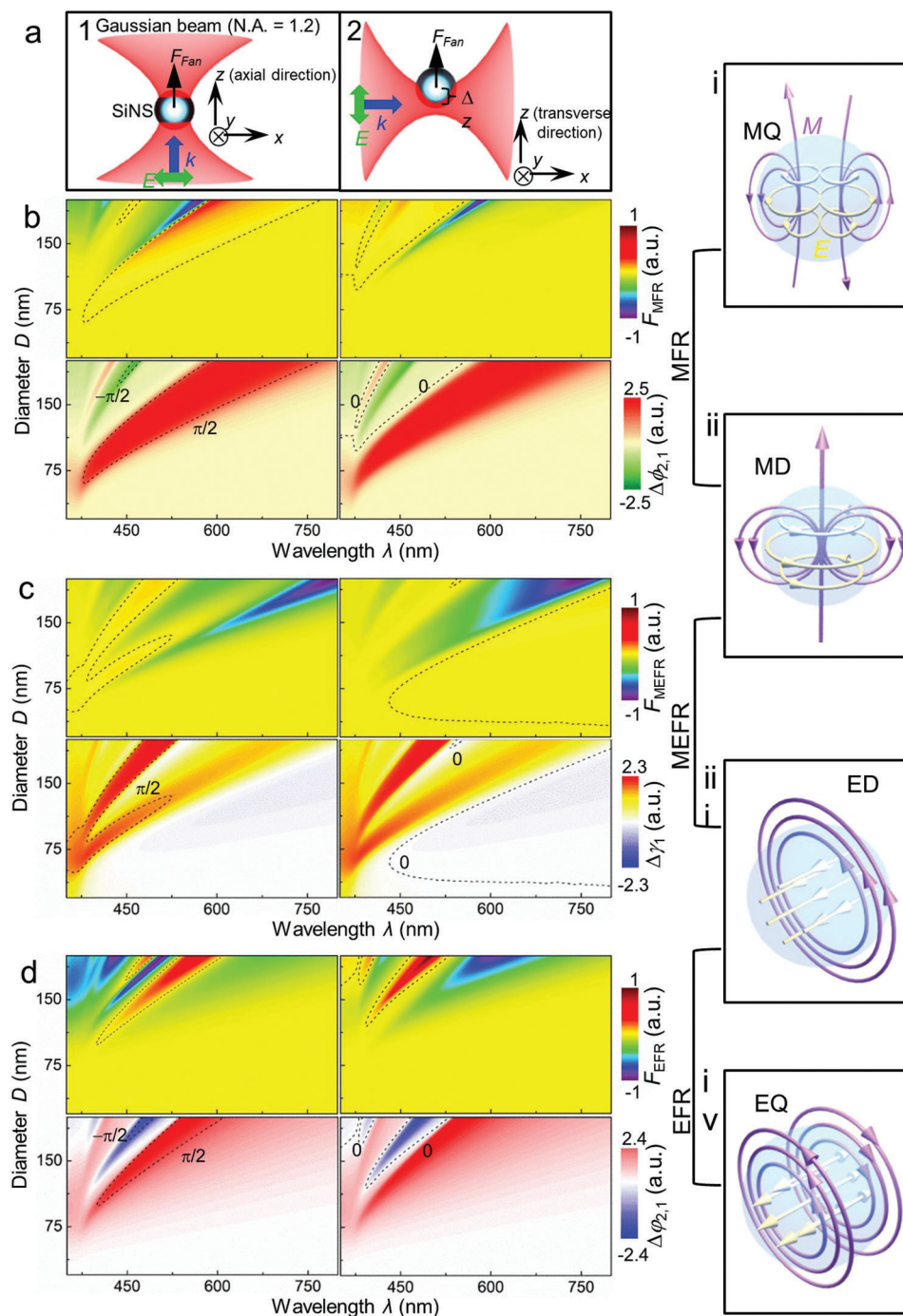


Figure 2. Dependence of the Fano-resonance-induced forces on the phase difference between interacting multipoles in the axial (left panels) and transverse (right panels) directions. a) Magnetic, b) magnetoelectric, and c) electric Fano-resonance-induced force and phase difference as a function of the light wavelength and the diameter of the SiNS. Black dashed lines demarcate the zero-force positions or specific values of the phase differences. Insets I and II show the illumination geometries used for calculation of the forces in the axial and transverse directions, respectively. Insets III–VI represent schematics of the multipoles inside the SiNS.

this case, the phase differences between the interacting multipoles for MFR, MEFR, and EFR are $\Delta\phi_{2,1}$, $\Delta\gamma_1$, and $\Delta\phi_{2,1}$, respectively.

In the axial direction, F_{MFR} is zero when the phase of MQ is orthogonal to that of MD (i.e., $\Delta\phi_{2,1} = \pm\pi/2$) (Figure 2a); F_{MFR} is

positive for $\Delta\phi_{2,1} > \pi/2$ or $\Delta\phi_{2,1} < -\pi/2$ and is negative for $-\pi/2 < \Delta\phi_{2,1} < \pi/2$ (Figure 2a). However, in the transverse direction, F_{MFR} vanishes for in-phase oscillations (i.e., $\Delta\phi_{2,1} = 0$), and is positive (or negative) for $\Delta\phi_{2,1} < 0$ (or $\Delta\phi_{2,1} > 0$). The sign of F_{MEFR} or F_{EFR} exhibits the same dependency on the phase difference

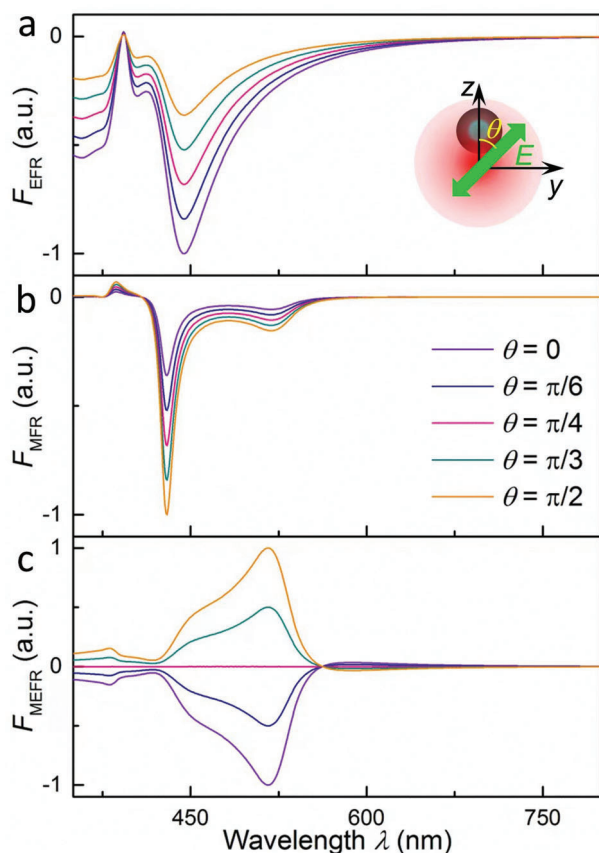


Figure 3. Polarization-dependent Fano-resonance-induced forces in the transverse direction. Transverse force spectra arising from the a) electric Fano resonance, b) magnetic Fano resonance, and c) magnetoelectric Fano resonance associated with different polarization directions θ .

as that of F_{MFR} (Figure 2b,c). Therefore, F_{MFR} , F_{MEFR} , and F_{EFR} are considered proportional to $\cos\Delta\phi_{2,1}$, $\cos\Delta\gamma_1$, and $\cos\Delta\phi_{2,1}$, respectively, in the axial direction, but proportional to $\sin\Delta\phi_{2,1}$, $\sin\Delta\gamma_1$, and $\sin\Delta\phi_{2,1}$, respectively, in the transverse direction. In addition, both illumination geometries (insets I and II) yield the same distribution of phase differences for MFR, MEFR, and EFR, indicating that the phase difference is insensitive to light intensity.

The polarization direction of the light is located in the transverse plane and therefore, owing to symmetry, should have no effect on the axial forces. However, we found that the transverse forces are strongly dependent on the polarization direction. **Figure 3** shows the transverse force spectra of a SiNS (diameter: $D = 120$ nm) obtained for different polarization directions θ ($0 \leq \theta \leq \pi/2$) with respect to the $+z$ direction (see the inset). The magnitude of F_{EFR} and F_{MFR} can be varied by changing θ . However, with the changes of θ , F_{EFR} and F_{MFR} are changed with a contrary tendency. The magnitude of F_{EFR} increases with increasing θ and is minimum and maximum at $\theta = 0$ and $\theta = \pi/2$, respectively (Figure 3a). In contrast, the magnitude of F_{MFR} decreases with increasing θ and is minimum and maximum at $\theta = \pi/2$ and $\theta = 0$, respectively (Figure 3b). For F_{MEFR} , both the sign and magnitude can be tuned by changing θ ; F_{MEFR} decreases with in-

creasing θ , vanishes for $\theta = \pi/4$, and is negative for $0 \leq \theta < \pi/4$ and positive for $\pi/4 < \theta \leq \pi/2$ (Figure 3c).

3. Discussion

As reported in previous studies,^[11–13,29–32] the optical force acting on a dipolar particle consists of two main components: a canonical radiation pressure and an intensity gradient force. The former is proportional to the optical orbital momentum (or phase gradient), whereas the gradient force is proportional to the light intensity gradient and can change its sign, when the light wavelength passes through the dipolar resonance. Therefore, forces acting on these particles are insensitive to the light polarization; also, the directions of these forces are expected to have only one turning point when changing the light wavelength or the size of the particle. In contrast, the directions of the Fano-resonance-induced forces have multiple turning points (Figure 2). Furthermore, the direction of F_{MEFR} as well as the magnitudes of F_{EFR} and F_{MFR} can be tuned by the polarization direction (Figure 3).

These unique characteristics of the Fano-resonance-induced forces would provide additional degrees of freedom for optical manipulation.^[33–37] For example, achieving controllable optical forces to actuate optomechanical devices is essential for levito-dynamics systems.^[38,39] Generally, the gradient force acts as the actuation force and, hence, the force, and therefore the devices, can be controlled by changing the light wavelength. Using Fano-resonant media as optomechanical devices may constitute a highly flexible optomechanical system, because the force can be controlled by changing the polarization direction, which (in practice) is more convenient than changing the light wavelength.

4. Conclusion

We have investigated the optical forces arising from the different types of Fano resonances in three dimensions using SiNSs as the Fano resonant media. Based on the types of interacting multipoles, the optical force associated with the Fano resonance can be written as the sum of three terms: the pure magnetic contribution (F_{MFR}), the pure electric contribution (F_{EFR}), and the contribution from magnetoelectric hybridization (F_{MEFR}). These three types of forces exhibit different relations with the polarization direction of light. In the transverse direction, the direction of F_{MEFR} can be tuned by light polarization. It is shown that light with orthogonal polarization directions can exert F_{MEFR} of opposite sense on the SiNS. The direction and magnitude of both F_{MFR} and F_{EFR} are invariant with and strongly dependent on, respectively, the polarization direction. The magnitudes of F_{EFR} and F_{MFR} decrease and increase, respectively, when the polarization direction deviates from the transversal displacement direction of the SiNS. The three types of forces have similar dependencies on the phase difference between the interacting multipoles. In the axial direction, each force is proportional to the cosine value of the phase difference between the multipoles, it is proportional to the sine value of the phase difference in the transverse direction. Based on these physical properties, the directions of these forces, in practice, can be tuned by changing the light wavelength and the size of the SiNS. The underlining physics is the significant phase variation near the multipolar resonance. When the light wavelength

passes through the resonance of one multipole, the phase of this multipole will vary significantly, whereas the phase of the other is almost maintained (Figure 1b). During this process, the two multipoles easily pass through a zero-phase difference or a $\pi/2$ -phase difference, leading to a change in the sign of the induced force in a certain (axial or transverse) direction. The understanding of Fano-based mechanical effects would facilitate new applications of Fano resonances in the field of optical manipulation and optomechanical systems.

Acknowledgements

Y.Z. and T.L. contributed equally to this work. The authors acknowledge financial support from the National Natural Science Foundation of China (nos. 11874183, 11621091, 11822406, 11834007, 11774164, and 11774162) and the National Program on Key Basic Research Project of China (2017YFA0303700). This work was also supported by the Fundamental Research Funds for the Central Universities (nos. 21621107 and 020414380175).

Conflict of Interest

The authors declare no conflict of interest.

Data Availability Statement

Data sharing is not applicable to this article as no new data were created or analyzed in this study.

Keywords

Mie-tronics, multipolar interplay, optical force, Si nanoparticles

Received: September 25, 2022

Revised: December 7, 2022

Published online:

- [1] A. García-Etxarri, R. Gómez-Medina, L. S. Froufe-Pérez, C. López, L. Chantada, F. Scheffold, J. Aizpurua, M. Nieto-Vesperinas, J. J. Sáenz, *Opt. Express* **2011**, *19*, 4815.
- [2] M. F. Limonov, *Adv. Opt. Photon.* **2021**, *13*, 703.
- [3] M. I. Tribelsky, B. S. Luk'yanchuk, *Phys. Rev. Lett.* **2006**, *97*, 263902.
- [4] M. Rahmani, B. Luk'yanchuk, M. Hong, *Laser Photonics Rev.* **2013**, *7*, 329.
- [5] X. Xu, M. Nieto-Vesperinas, *Phys. Rev. Lett.* **2019**, *123*, 233902.
- [6] D. A. Kislov, E. A. Gurvitz, V. Bobrovs, A. A. Pavlov, D. N. Redka, M. I. Marqués, P. Ginzburg, A. S. Shalin, *Adv. Photon. Res.* **2021**, *2*, 2100082.

- [7] X. Xu, M. Nieto-Vesperinas, C.-W. Qiu, X. Liu, D. Gao, Y. Zhang, B. Li, *Laser Photon. Rev.* **2020**, *14*, 1900265.
- [8] H. Wang, P. Liu, Y. Ke, Y. Su, L. Zhang, N. Xu, S. Deng, H. Chen, *ACS Nano* **2015**, *9*, 436.
- [9] J. Olmos-Trigo, C. Sanz-Fernández, D. R. Abujetas, J. Lasa-Alonso, N. de Sousa, A. García-Etxarri, J. A. Sánchez-Gil, G. Molina-Terriza, J. J. Sáenz, *Phys. Rev. Lett.* **2020**, *125*, 073205.
- [10] A. Kiselev, K. Achouri, O. J. F. Martin, *Opt. Express* **2020**, *28*, 27547.
- [11] Y. Zhou, X. Xu, Y. Zhang, M. Li, S. Yan, M. Nieto-Vesperinas, B. Li, C.-W. Qiu, B. Yao, *Proc. Natl. Acad. Sci. USA* **2022**, *119*, e2209721119.
- [12] K. Y. Bliokh, A. Y. Bekshaev, F. Nori, *Nat. Commun.* **2014**, *5*, 3300.
- [13] A. Y. Bekshaev, K. Y. Bliokh, F. Nori, *Phys. Rev. X* **2015**, *5*, 011039.
- [14] M. Nieto-Vesperinas, X. Xu, *Phys. Rev. Res.* **2021**, *3*, 043080.
- [15] H. Chen, L. Feng, J. Ma, C. Liang, Z. Lin, H. Zheng, *Phys. Rev. B* **2022**, *106*, 054301.
- [16] H. Chen, Q. Ye, Y. Zhang, L. Shi, S. Liu, Z. Jian, Z. Lin, *Phys. Rev. A* **2017**, *96*, 023809.
- [17] H. Chen, S. Liu, J. Zi, Z. Lin, *ACS Nano* **2015**, *9*, 1926.
- [18] A. Devi, B. Sikdar, A. K. De, *Phys. Rev. A* **2022**, *105*, 053529.
- [19] A. Devi, A. K. De, *Phys. Rev. A* **2020**, *102*, 023509.
- [20] A. Devi, A. K. De, *Phys. Rev. Res.* **2020**, *2*, 043378.
- [21] X. Xu, C. Cheng, Y. Zhang, H. Lei, B. Li, *J. Phys. Chem. Lett.* **2016**, *7*, 314.
- [22] M. A. Green, M. J. Keevers, *Prog. Photovolt. Res. Appl.* **1995**, *3*, 189.
- [23] M. I. Mishchenko, L. D. Travis, A. A. Lacis, *Scattering, Absorption, and Emission of 480 Light by Small Particles*, Cambridge University Press, Cambridge, UK **2002**.
- [24] J. D. Jackson, *Classical Electrodynamics*, Wiley, New York **1962**.
- [25] M. Nieto-Vesperinas, X. Xu, *Light Sci. Appl.* **2022**, *11*, 297.
- [26] J. P. Barton, D. R. Alexander, S. A. Schaub, *J. Appl. Phys.* **1989**, *66*, 4594.
- [27] J. Olmos-Trigo, D. R. Abujetas, C. Sanz-Fernandez, J. A. Sanchez-Gil, J. J. Sáenz, *Phys. Rev. Res.* **2020**, *2*, 013225.
- [28] C. Sanz-Fernández, M. Molezuelas-Ferreras, J. Lasa-Alonso, N. de Sousa, X. Zambrana-Puyalto, J. Olmos-Trigo, *Laser Photon. Rev.* **2021**, *15*, 2100035.
- [29] P. C. Chaumet, M. Nieto-Vesperinas, *Opt. Lett.* **2000**, *25*, 1065.
- [30] S. Albaladejo, M. I. Marqués, M. Laroche, J. J. Sáenz, *Phys. Rev. Lett.* **2009**, *102*, 113602.
- [31] D. B. Ruffner, D. G. Grier, *Phys. Rev. Lett.* **2013**, *111*, 059301.
- [32] M. I. Marqués, J. J. Sáenz, *Phys. Rev. Lett.* **2013**, *111*, 059302.
- [33] M. Nieto-Vesperinas, J. J. Sáenz, R. Gómez-Medina, L. Chantada, *Opt. Express* **2010**, *18*, 11428.
- [34] T. Li, X. Xu, B. Fu, S. Wang, B. Li, Z. Wang, S. Zhu, *Photon. Res.* **2021**, *9*, 1062.
- [35] X. Xu, Y. Yang, L. Chen, X. Chen, T. Wu, Y. Li, X. Liu, Y. Zhang, B. Li, *Laser Photon. Rev.* **2021**, *15*, 2000546.
- [36] M. Li, X. Chen, S. Yan, Y. Zhang, B. Yao, *Adv. Photon. Res.* **2022**, *3*, 2200117.
- [37] T. Li, J. J. Kingsley-Smith, Y. Hu, X. Xu, S. Yan, S. Wang, B. Yao, Z. Wang, S. Zhu, *Opt. Lett.* <https://doi.org/10.1364/OL.478979>
- [38] Y. Hu, J. J. Kingsley-Smith, M. Nikkhou, J. A. Sabin, F. J. Rodríguez-Fortuño, X. Xu, J. Millen, (Preprint) arXiv:2209.09759, v1, submitted: Sept **2022**.
- [39] J. Millen, T. S. Monteiro, R. Pettit, A. N. Vamivakas, *Rep. Prog. Phys.* **2020**, *83*, 026401.